

Original article

Hydrazones of 1,2-benzisothiazole hydrazides: synthesis, antimicrobial activity and QSAR investigations

Paola Vicini ^{a,*}, Franca Zani ^a, Pietro Cozzini ^b, Irini Doytchinova ^c^a Dipartimento Farmaceutico, Università degli Studi di Parma, Parco Area delle Scienze 27/A, 43100 Parma, Italy^b Dipartimento di Chimica Generale ed Inorganica, Chimica Analitica, Chimica Fisica, Parco Area delle Scienze 17/A, 43100 Parma, Italy^c Edward Jenner Institute for Vaccine Research, Compton, Berkshire RG20 7NN, UK

Received 21 December 2001; accepted 19 March 2002

Abstract

A series of hydrazones of 1,2-benzisothiazole hydrazides **1a–m**, **2a–m**, **3a–m**, **4a–m**, **5a–m** as well as their cyclic (**1** and **4**) and acyclic (**2**, **3** and **5**) 1,2-benzisothiazole parent hydrazides, were synthesised and evaluated as antibacterial and antifungal agents. All of the 2-amino-1,2-benzisothiazol-3(2H)-one derivatives, belonging to series **I** and **IV**, showed a good antibacterial activity against Gram positive bacteria. Most of them were active against yeasts too. Compounds **1** and **4**, together with **1l**, proved to be the most effective compounds. Quantitative structure-activity relationship (QSAR) investigation with a 2D-QSAR analysis was applied to find a correlation between different experimental or calculated physicochemical parameters of the compounds studied. A 3D-QSAR study was performed, applying Comparative Molecular Similarity Indices Analysis (CoMSIA) method, to derive quantitative models relating the structural features of 1,2-benzisothiazole derivatives **1**, **1a–m** and **4**, **4a–m** and their antimicrobial activity against *Bacillus subtilis*, resulted the most sensitive micro-organism. © 2002 Éditions scientifiques et médicales Elsevier SAS. All rights reserved.

Keywords: 1,2-Benzisothiazol-3(2H)-one; Hydrazones; Antibacterial activity; Antifungal activity; QSAR; CoMSIA

1. Introduction

Pursuing our studies on 1,2-benzisothiazole derivatives with antibacterial and antifungal activity [1–3], as a part of a research project on hydrazones of 1,2-benzisothiazole hydrazides with potential antimicrobial activity, we recently reported [4] the synthesis and the correlation between experimental and calculated lipophilic indices of new compounds belonging to the five series **I–V** (Table 1).

Since it is well known that the hydrazone group plays an important role for the antimicrobial activity [5–9] and a number of 1,2-benzisothiazole derivatives have been claimed to possess interesting antibacterial and antifungal activities [10–12], in the present paper we report the evaluation of the in vitro antimicrobial activity of compounds belonging to series **I–V** (Table 1) and the investigation of the relationship between their physicochemical properties and microbiological effects.

Several studies have pointed out the major role of lipophilicity in antimicrobial activity [13,14] and in particular it has already been suggested [15,16] that a mode of action of 1,2-benzisothiazol-3(2H)-one derivatives with antibacterial activity involves an unspecific interaction (strictly related to the hydrophobic character of the molecules) on protein thiol groups. Moreover, concerning antifungal activity, many compounds exert a membrane action, strictly related to lipophilicity [17,18]. For the above considerations we decided to look for a correlation between lipophilicity parameters [4] of benzisothiazole hydrazones and their antimicrobial activity. Following general antimicrobial screening, indicating sufficiently encouraging effects, two series (**I** and **IV**) were selected for an extensive evaluation of their antimicrobial effects against representative bacterial and fungal micro-organisms.

Therefore, to complete our study, we have performed a quantitative structure-activity relationship (QSAR) investigation in order to reach a fuller understanding of the importance of the different physicochemical

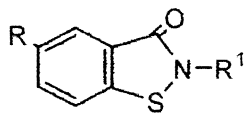
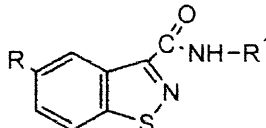
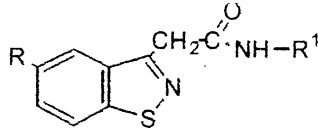

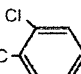
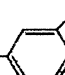

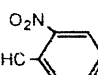
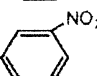
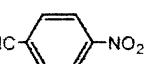
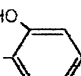
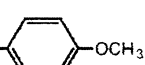
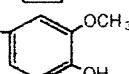
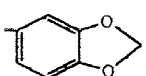
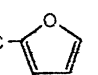
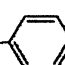
* Correspondence and reprints

E-mail address: pvicini@ipruniv.cce.unipr.it (P. Vicini).

properties. In principle, the QSAR analysis is based on the assumption that the structurally similar compounds are similarly oriented and bind to the same biological target noncovalently. The different QSAR techniques

differ in the way they describe the compounds and in how they detect the relationship between structure and activity. The aim of the two-dimensional (2D) QSAR studies is to find a correlation between different experimental or

Table 1
Structures of the compounds under study

					
	I R=H	IV R=CH₃	II R=H	III R=H	V R=CH₃
R¹ =					
–NH₂	1	4	2	3	5
–N=HC– 	1a	4a	2a	3a	5a
–N=HC– 	1b	4b	2b	3b	5b
–N=HC– 	1c	4c	2c	3c	5c
–N=HC– 	1d	4d	2d	3d	5d
–N=HC– 	1e	4e	2e	3e	5e
–N=HC– 	1f	4f	2f	3f	5f
–N=HC– 	1g	4g	2g	3g	5g
–N=HC– 	1h	4h	2h	3h	5h
–N=HC– 	1i	4i	2i	3i	5i
–N=HC– 	1j	4j	2j	3j	5j
–N=HC– 	1k	4k	2k	3k	5k
–N=HC– 	1l	4l	2l	3l	5l
–N=HC–CH=CH– 	1m	4m	2m	3m	5m

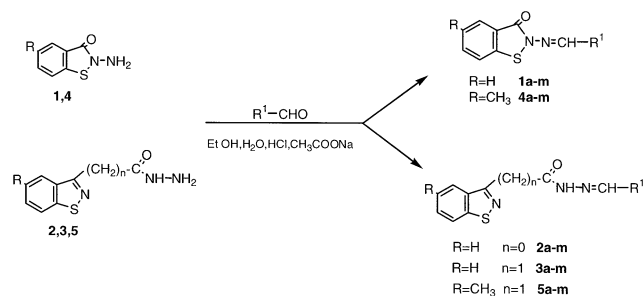


Fig. 1. General scheme for synthesis of 1,2-benzisothiazole hydrazones **1a–m**, **2a–m**, **3a–m**, **4a–m**, **5a–m**.

Table 2
Physicochemical data of compounds **1–1m**

	Analyses (C, H, N)	MW	M.p. (°C)	Yield (%)
1	$C_7H_6N_2OS$ [4]	166.21	138–141 ^a	70
1a	$C_{14}H_{10}N_2OS$ [22]	254.31	195–196	76
1b	$C_{14}H_9ClN_2OS$	288.75	218–219	76
1c	$C_{14}H_9ClN_2OS$	288.75	221–223	57
1d	$C_{14}H_9ClN_2OS$	288.75	207–211	76
1e	$C_{14}H_9N_3O_3S$	299.30	234–235	78
1f	$C_{14}H_9N_3O_3S$	299.30	253–254	72
1g	$C_{14}H_9N_3O_3S$	299.30	270–271	83
1h	$C_{14}H_{10}N_2O_2S$	270.31	241–242 ^b	75
1i	$C_{15}H_{12}N_2O_2S$	284.34	175–177	82
1j	$C_{15}H_{12}N_2O_3S$	300.33	208–210	72
1k	$C_{15}H_{10}N_2O_3S$	298.33	215–218	66
1l	$C_{12}H_9N_2O_2S$	245.29	160–162	84
1m	$C_{16}H_{12}N_2OS$	280.34	158–160	80

^a Crystallized from water.

^b Crystallized from dioxan.

Table 3
Physicochemical data of compounds **4–4m**

	Analyses (C, H, N)	MW	M.p. (°C)	Yield (%)
4	$C_8H_8N_2OS$ [22]	180.22	154–156 ^a	75
4a	$C_{15}H_{12}N_2OS$ [22]	268.33	204–205	70
4b	$C_{15}H_{11}ClN_2OS$	302.79	193–195	87
4c	$C_{15}H_{11}ClN_2OS$	302.79	201–203	79
4d	$C_{15}H_{11}ClN_2OS$	302.79	201–203	79
4e	$C_{15}H_{11}N_3O_3S$	313.33	248–250 ^b	82
4f	$C_{15}H_{11}N_3O_3S$	313.33	238–240 ^b	88
4g	$C_{15}H_{11}N_3O_3S$	313.33	274–275 ^b	77
4h	$C_{15}H_{12}N_2O_2S$	284.34	240–242 ^b	88
4i	$C_{16}H_{14}N_2O_2S$	298.37	198–200	75
4j	$C_{16}H_{14}N_2O_3S$	314.36	206–208	75
4k	$C_{16}H_{12}N_2O_3S$	312.35	222–224	88
4l	$C_{13}H_{10}N_2O_2S$	258.29	159–161	63
4m	$C_{17}H_{14}N_2OS$	294.37	195–196	89

^a Crystallized from water.

^b Crystallized from dioxan.

calculated physicochemical parameters of the compounds and their biological activity. Three-dimensional (3D) QSARs are quantitative models that relate the activity of molecules with their properties calculated in

3D space. The 3D-QSAR method Comparative Molecular Similarity Indices Analysis (CoMSIA) calculates indices of similarity in the 3D space surrounding each of the aligned molecules and correlates them with the activities of the studied compounds [19–21]. The greatest advantage of the 3D-QSAR methods is their ability to visualise the areas that ‘favour’ or ‘disfavour’ the presence of a group with a particular physicochemical property.

In the present study 2D- and 3D-QSAR methods were applied to derive quantitative models relating the structural features of 1,2-benzisothiazole derivatives **1**, **1a–m** and **4**, **4a–m** and their antimicrobial activity. Besides the explanatory ability of these models, they could be used to predict the potency of compounds not yet tested and to suggest ideas for further synthesis of new molecules with enhanced activity.

2. Chemistry

The hydrazones **1a–m**, **2a–m**, **3a–m**, **4a–m**, **5a–m** (Table 1) were synthesised from cyclic (**1** and **4**) or acyclic (**2**, **3** and **5**) 1,2-benzisothiazole hydrazides. Condensation of the appropriate hydrazide with aldehydes, in ethanolic mixture and at a buffered pH, afforded the title compounds (Fig. 1). The substituents on the aldehyde moiety were chosen introducing different groups, such as NO_2 , or elements (Cl), which can be assumed to confer antimicrobial activity. In addition to the different hydrophobicity of the substituents, the five different series were designed such that the hydrophobicity varied also among congeners. The detailed conditions for preparing the intermediate hydrazides **1–5** are reported in our previous works [4,22].

Physicochemical and spectroscopic characterisation of the hydrazides **1–5** and of hydrazones **2a–m**, **3a–m** and **5a–m** as well as of compounds **1a** and **4a** have been previously described [4,22].

The compounds **1b–m** and **4b–m**, here newly described, were obtained in generally good yields (70–90%) and purified by recrystallisation, using ethanol (unless otherwise noted). Physicochemical data of these compounds are shown in Tables 2 and 3. Elemental analysis, for C, H, N, were within the range $\pm 0.4\%$ of theoretical values. Structural 1H -NMR and IR data have only been given in the Experimental protocols for compound **1b**. Complete data can be obtained from the authors on request.

3. Biology

The in vitro antimicrobial activity of the synthesised compounds was assayed on bacterial and fungal strains reported in Tables 4 and 6. The minimum inhibitory

concentration (MIC) was determined by the two-fold dilution technique. Ampicillin and miconazole were employed during the test procedures as references.

To establish the microbistatic or microbicidal kind of the exerted inhibition, the minimum bactericidal concentrations (MBC) and the minimum fungicidal concentrations (MFC) were detected (Table 5).

4. Results

4.1. Antimicrobial activity

The MIC values obtained for hydrazones **1a–m** and **4a–m** as well as for their parents 2-amino-1,2-benzisothiazol-3(2H)-ones **1** and **4** are reported in Table 4. 1,2-Benzisothiazolyldrazides **2**, **3** and **5** and their hydrazone derivatives **2a–m**, **3a–m** and **5a–m** were tested and found inactive (MIC values $>100 \mu\text{g mL}^{-1}$).

All the compounds reported in Table 4 showed a good antibacterial activity against Gram positive bacteria. *Bacillus subtilis* (BS) was found to be more sensitive than *Staphylococcus aureus* (SA). Compounds **1** and **4** proved to be the most effective, having a MIC value of $0.7 \mu\text{g mL}^{-1}$ against *B. subtilis*; these compounds, together with **1l**, were the only ones also active against Gram negative bacteria (*Escherichia coli*, MIC $6\text{--}25 \mu\text{g mL}^{-1}$). In all cases the assayed substances showed an activity level against bacteria lower than that of ampicillin, the reference drug.

Many of the tested benzisothiazolones showed antifungal properties, displaying MIC values of $6\text{--}25 \mu\text{g mL}^{-1}$ against *Saccharomyces cerevisiae* (SC) and *Candida tropicalis*. Compounds **1**, **1l** and **4** were also active against *Aspergillus niger*. Some substances displayed a growth inhibition (MIC $6 \mu\text{g mL}^{-1}$) against yeasts higher or comparable to that of miconazole, the reference drug.

Table 4

Antimicrobial activity, expressed as MIC ($\mu\text{g mL}^{-1}$) and, in brackets, as $-\log \text{MIC}$ (mol L $^{-1}$)

Compound	Bacteria ^a			Fungi ^b		
	BS	SA	EC	SC	CT	AN
1	0.7 (5.376)	6 (4.442)	6 (4.442)	6 (4.442)	6 (4.442)	100 (3.221)
1a	6 (4.627)	12 (4.326)	>100 (n.c.) ^c	6 (4.627)	6 (4.627)	>100 (n.c.)
1b	6 (4.682)	12 (4.381)	>100 (n.c.)	>100 (n.c.)	>100 (n.c.)	>100 (n.c.)
1c	6 (4.682)	>100 (n.c.)	>100 (n.c.)	>100 (n.c.)	>100 (n.c.)	>100 (n.c.)
1d	3 (4.983)	12 (4.381)	>100 (n.c.)	6 (4.682)	>100 (n.c.)	>100 (n.c.)
1e	12 (4.397)	25 (4.078)	>100 (n.c.)	>100 (n.c.)	>100 (n.c.)	>100 (n.c.)
1f	6 (4.698)	50 (3.777)	>100 (n.c.)	>100 (n.c.)	>100 (n.c.)	>100 (n.c.)
1g	6 (4.698)	>100 (n.c.)	>100 (n.c.)	>100 (n.c.)	>100 (n.c.)	>100 (n.c.)
1h	6 (4.654)	12 (4.353)	>100 (n.c.)	25 (4.034)	>100 (n.c.)	>100 (n.c.)
1i	6 (4.676)	12 (4.375)	>100 (n.c.)	6 (4.676)	12 (4.375)	>100 (n.c.)
1j	6 (4.699)	25 (4.080)	>100 (n.c.)	12 (4.398)	>100 (n.c.)	>100 (n.c.)
1k	3 (4.998)	12 (4.396)	>100 (n.c.)	6 (4.716)	>100 (n.c.)	>100 (n.c.)
1l	6 (4.612)	12 (4.310)	25 (3.992)	6 (4.612)	12 (4.310)	25 (3.992)
1m	6 (4.670)	12 (4.369)	>100 (n.c.)	6 (4.670)	12 (4.369)	>100 (n.c.)
4	0.7 (5.411)	6 (4.478)	25 (3.858)	6 (4.478)	12 (4.177)	50 (3.557)
4a	6 (4.651)	12 (4.349)	>100 (n.c.)	6 (4.651)	>100 (n.c.)	>100 (n.c.)
4b	6 (4.703)	>100 (n.c.)	>100 (n.c.)	>100 (n.c.)	>100 (n.c.)	>100 (n.c.)
4c	3 (5.004)	>100 (n.c.)	>100 (n.c.)	>100 (n.c.)	>100 (n.c.)	>100 (n.c.)
4d	3 (5.004)	12 (4.402)	>100 (n.c.)	6 (4.703)	>100 (n.c.)	>100 (n.c.)
4e	12 (4.417)	>100 (n.c.)	>100 (n.c.)	>100 (n.c.)	>100 (n.c.)	>100 (n.c.)
4f	6 (4.718)	12 (4.417)	>100 (n.c.)	>100 (n.c.)	>100 (n.c.)	>100 (n.c.)
4g	12 (4.417)	>100 (n.c.)	>100 (n.c.)	>100 (n.c.)	>100 (n.c.)	>100 (n.c.)
4h	6 (4.676)	12 (4.375)	>100 (n.c.)	>100 (n.c.)	>100 (n.c.)	>100 (n.c.)
4i	25 (4.077)	50 (3.776)	>100 (n.c.)	>100 (n.c.)	>100 (n.c.)	>100 (n.c.)
4j	6 (4.719)	25 (4.099)	>100 (n.c.)	6 (4.719)	>100 (n.c.)	>100 (n.c.)
4k	3 (5.018)	12 (4.415)	>100 (n.c.)	>100 (n.c.)	>100 (n.c.)	>100 (n.c.)
4l	6 (4.634)	12 (4.333)	>100 (n.c.)	6 (4.634)	12 (4.333)	>100 (n.c.)
4m	6 (4.691)	25 (4.071)	>100 (n.c.)	6 (4.691)	>100 (n.c.)	>100 (n.c.)
Ampicillin	0.015	0.15	3	— ^d	—	—
Miconazole	—	—	—	12	6	3

^a Gram positive bacteria: *B. subtilis* ATCC 6633 (BS) and *S. aureus* ATCC 25923 (SA); Gram negative bacteria: *E. coli* SPA 27 (EC).

^b Yeasts: *S. cerevisiae* ATCC 9763 (SC) and *C. tropicalis* ATCC 1369 (CT); mould: *A. niger* ATCC 6275 (AN).

^c Not calculated because MIC value is higher than $100 \mu\text{g mL}^{-1}$.

^d Not tested.

Table 5
Antimicrobial activity, expressed as MBC and MFC ($\mu\text{g mL}^{-1}$)

Compound	Bacteria ^a			Fungi ^b		
	BS	SA	EC	SC	CT	AN
1	1.5	12	50	25	25	>100
1a	12	100	– ^c	12	100	–
1b	25	>100	–	–	–	–
1c	12	–	–	–	–	–
1d	25	100	–	12	–	–
1e	25	>100	–	–	–	–
1f	50	>100	–	–	–	–
1g	50	–	–	–	–	–
1h	12	>100	–	100	–	–
1i	25	>100	–	12	>100	–
1j	25	>100	–	>100	–	–
1k	6	>100	–	12	–	–
1l	12	50	>100	12	25	>100
1m	12	>100	–	12	25	–
4	1.5	25	100	12	25	>100
4a	25	100	–	12	–	–
4b	25	–	–	–	–	–
4c	50	–	–	–	–	–
4d	25	>100	–	12	–	–
4e	25	–	–	–	–	–
4f	25	>100	–	–	–	–
4g	>100	–	–	–	–	–
4h	12	>100	–	–	–	–
4i	>100	>100	–	–	–	–
4j	25	>100	–	12	–	–
4k	12	>100	–	–	–	–
4l	12	50	–	12	100	–
4m	25	>100	–	12	–	–

^a Gram positive bacteria: *B. subtilis* ATCC 6633 (BS) and *S. aureus* ATCC 25923 (SA); Gram negative bacteria: *E. coli* SPA 27 (EC).

^b Yeasts: *S. cerevisiae* ATCC 9763 (SC) and *C. tropicalis* ATCC 1369 (CT); mould: *A. niger* ATCC 6275 (AN).

^c Not tested because MIC value is higher than $100 \mu\text{g mL}^{-1}$.

All the tested compounds exhibited, against the used micro-organisms, microbistatic activity: the MBC and MFC values were two to 16 times higher than MIC values (Table 5).

Compounds **1**, **1l** and **4**, the most effective antimicrobial substances displaying growth inhibition of all the tested micro-organisms, were further investigated for their activity against a number of different Gram positive and Gram negative bacteria, yeasts and moulds. The results, reported in Table 6, point out that compound **1** shows a strong activity against many Gram positive bacteria, such as several bacilli, *Sarcina lutea*, *Staphylococcus epidermidis*, *Streptococcus faecalis*, at concentrations of $0.3\text{--}1.5 \mu\text{g mL}^{-1}$. A good activity was exhibited by compound **1** also against Gram negative bacteria with MIC $1.5\text{--}12 \mu\text{g mL}^{-1}$ and yeasts (*Candida* spp., *Cryptococcus neoformans*) with MIC $12\text{--}50 \mu\text{g mL}^{-1}$.

Against the same Gram positive bacteria, compound **4** displayed an inhibitory activity identical with that of

compound **1** (MIC $0.3\text{--}1.5 \mu\text{g mL}^{-1}$; table not shown). Moreover, compound **1l** was endowed with interesting antifungal properties against moulds including *Aspergillus flavus* (MIC $100 \mu\text{g mL}^{-1}$), *Pseudallescheria boydii* (MIC $25 \mu\text{g mL}^{-1}$), *Sporothrix schenckii* (MIC $12 \mu\text{g mL}^{-1}$) and dermatophytes. Among the last ones, *Trichophyton rubrum* and *T. soudanense* were remarkably inhibited at the concentration of $3 \mu\text{g mL}^{-1}$, *T. mentagrophytes* and *Epidermophyton floccosum* at $6 \mu\text{g mL}^{-1}$, *T. interdigitalis* at $12 \mu\text{g mL}^{-1}$ and *Microsporum gypseum* at $25 \mu\text{g mL}^{-1}$.

4.2. Structure–activity relationships

4.2.1. 2D-QSAR study

The antimicrobial activities of the compounds studied, presented in *p*-units ($-\log \text{MIC mol L}^{-1}$) (Table 4), were used in the 2D- and 3D-QSAR studies. For the purposes of 2D-QSAR the chemical structure of the compounds was described by three groups of parameters: steric, electrostatic and hydrophobic. As steric parameters were included the molecular volume MVol, the diameters of the ellipsoid occupied by the molecules, axis *A* and axis *B*, and the solvent accessible surface area SASA. Molecular volume is computed using GRASP software, kindly supplied by the authors [23]; axis *A* and axis *B* are the major and minor axis of a hypothetical ellipsoid defined by molecular surface. The dipole and the partial charges at some of the main atoms (q_{O} , q_{S} , q_{Nring} and $q_{\text{N'}}$) were applied as parameters describing the electron density in the molecules. As N' was signed the nitrogen atom involved in the N=C double bond. The hydrophobicity was described by $\log P_{\text{calc}}$ and some RP-HPLC parameters derived in our previous study [4] ($\log k'_{55}$, $\log k'_{80}$ and $\log k'_{\text{w}}$). An indicator variable I_{CH_3} was included in the study to distinguish between **1a–m** and **4a–m**. The principal component analysis (PCA) showed that four principal components (PC) explained 95% of the variance in the chemical structure. Table 7 presents the correlation matrix of the antimicrobial activity, PC scores and 2D parameters of the studied benzisothiazoles. Due to many missing values the matrix contained only 12 observations.

4.2.2. 3D-QSAR study

As the compounds represent two flat structures connected by three flexible bonds, the number of the low-energy conformers were 8 (2^3) (Table 8). Eight sets of compounds were built, optimised using molecular mechanics (MM) and the partial atomic charges were computed by AM1 semiempirical method. The different alignments were compared according to their q^2 values and standard errors of prediction (SEP) of the all fields model. Since only the combination of all fields provides full insight into the spatial features of the contribution

of different fields, the all fields model was considered in the initial analysis. The initial settings were grid spacing of 2.0 Å, attenuating factor $\alpha = 0.3$ and column filtering 2.0. Models for activity against BS, SA and SC were tested. Not enough data different from MIC > 100 $\mu\text{g mL}^{-1}$ were available for the other activities. Significant results (positive q^2 values) were found only for BS inhibition. Alignment 4 showed the highest value for q^2 and the lowest SEP (Table 8). This model was used in all further analyses.

There are a number of parameters in CoMSIA that can be set by the user so as to influence the final results. The BS all fields model was calibrated according to the grid spacing step, attenuating factor α and column filtering σ_{\min} . The highest q^2 value (0.592) was found at grid box step of 2.5 Å, α equal to 0.9 and σ_{\min} threshold fixed at 3.0. These settings were used in the further analyses.

The low number of components (only two) indicated that some of the fields used in the all fields model showed one and the same trends in the structure–activity relationship. To examine the contribution of each field, single field CoMSIA models were generated and combined in a stepwise manner. The single field models revealed the leading role of the steric field, followed by

the hydrophobic and H-bond donor ones (Table 9). The negative q^2 value for the acceptor field explained its negative interference on the all fields model. The combination between the remaining four fields gave the highest q^2 and r^2 values found in this study. To avoid any chance correlation this model was tested by cross-validation (CV) in two groups (20 runs) and by bootstrap analysis (20 runs). The close values for q^2_{LHO} and q^2_{LOO} as well as for r^2 and $r^2_{\text{bootstrap}}$ were indicative for the stability of this four fields model. This model was used to display the coefficient contour maps.

The maps of the four physicochemical properties having positive contribution to the antimicrobial activity against BS are presented in Fig. 2. The aligned structures are shown inside the different fields. The fields are considered in the order of their significance for the activity. Disfavoured areas in the hydrophobic and hydrogen-bond acceptor maps have been not displayed at the accepted level (-0.005).

Bulky substituents are favoured at *o*- and *m*-positions of the phenyl ring (Fig. 2, upper left). Another green area exists near the second *o*-position. Bulky substituents are disfavoured at *p*-position. There is only one area in the hydrogen-bond donor map (Fig. 2, upper right). This is a preferred hydrogen-bond donor

Table 6
Antimicrobial activity of compound **1** against several Gram positive and Gram negative bacteria and yeasts (MIC, $\mu\text{g mL}^{-1}$)

Micro-organism (number of clinical isolates)	Compound 1	Ampicillin	Miconazole
Gram positive bacteria			
<i>B. brevis</i> BGSC 26A1	0.3	100	— ^a
<i>B. cereus</i> ATCC 11966	1.5	100	—
<i>B. circulans</i> BGSC 16A1	0.3	3	—
<i>B. megaterium</i> BGSC 7A2	1.5	0.15	—
<i>B. pumilus</i> BGSC 8E2	1.5	0.07	—
<i>B. subtilis</i> var. <i>natto</i> BGSC 27A1	1.5	0.03	—
<i>B. thuringiensis</i> var. <i>kurstaki</i> BGSC 4D1	1.5	>100	—
<i>B. thuringiensis</i> var. <i>thuringiensis</i> BGSC 4B1	1.5	100	—
<i>S. lutea</i> ATCC 9341	0.7	0.003	—
<i>S. epidermidis</i> ATCC 12228	1.5	25	—
<i>S. faecalis</i> (n.1)	1.5	0.7	—
Gram negative bacteria			
<i>Enterobacter cloacae</i> ATCC 23355	12	>100	—
<i>Klebsiella pneumoniae</i> (n. 1)	12	100	—
<i>Proteus vulgaris</i> ATCC 13315	1.5	0.3	—
<i>Pseudomonas aeruginosa</i> ATCC 9027	100	100	—
<i>Pseudomonas cepacia</i> ATCC 25609	3	>100	—
<i>Salmonella typhimurium</i> ATCC 14028	12	1.5	—
<i>Serratia marcescens</i> ATCC 8100	12	>100	—
Yeasts			
<i>C. albicans</i> ATCC 10231	50	—	6
<i>C. albicans</i> (n. 3)	50	—	6
<i>C. guilliermondii</i> (n. 2)	12	—	0.3
<i>C. parapsilosis</i> (n. 2)	12	—	0.7
<i>C. tropicalis</i> (n. 1)	25	—	3
<i>C. neoformans</i> (n.1)	12	—	0.3

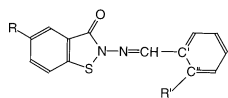
^a Not tested.

Table 7
Correlation matrix of antimicrobial activity, principal components scores and physicochemical parameters, $n = 12$

	BS	SA	SC	PC1	PC2	PC3	PC4	MVol	Axis A	Axis B	SASA	Dipole	q_O	q_S	q_{Nring}	$q_{N'}$	$\log P_{calc}$	$\log k'_{55}$	$\log k'_w$	$\log k'_{80}$	I_{CH3}
BS	1.000																				
SA	0.581	1.000																			
SC	-0.071	0.153	1.000																		
PC1	-0.703	-0.472	0.236	1.000																	
PC2	-0.069	-0.349	-0.510	0.000	1.000																
PC3	-0.203	-0.003	0.734	0.000	0.000	1.000															
PC4	0.160	0.200	0.024	0.000	0.000	0.000	1.000														
MVol	-0.720	-0.551	0.203	0.920	0.247	0.143	0.145	1.000													
Axis A	-0.799	-0.428	0.336	0.908	0.034	0.197	0.032	0.962	1.000												
Axis B	-0.174	-0.867	-0.400	0.161	0.670	-0.298	0.459	0.354	0.136	1.000											
SASA	-0.766	-0.552	0.244	0.934	0.200	0.155	0.130	0.996	0.978	0.314	1.000										
Dipole	0.432	-0.270	0.175	-0.053	0.683	0.269	0.261	-0.232	-0.340	0.432	-0.242	1.000									
q_O	0.463	0.100	-0.623	-0.296	0.568	0.683	-0.273	-0.222	-0.351	0.297	-0.286	0.116	1.000								
q_S	-0.780	-0.452	0.256	0.651	0.204	-0.611	-0.076	0.626	0.693	0.026	0.670	-0.320	-0.629	1.000							
q_{Nring}	0.908	0.597	-0.097	-0.906	-0.307	0.016	0.072	-0.908	-0.931	-0.272	-0.929	0.364	0.284	-0.803	1.000						
$q_{N'}$	-0.890	-0.540	0.297	0.935	0.126	-0.166	0.003	0.877	0.927	0.153	0.911	-0.313	-0.541	0.899	-0.952	1.000					
$\log P_{calc}$	-0.598	-0.123	0.486	0.880	-0.282	0.113	-0.136	0.747	0.825	-0.174	0.775	-0.276	-0.350	0.612	-0.738	0.753	1.000				
$\log k'_{55}$	-0.617	-0.147	0.375	0.915	-0.283	0.127	-0.064	0.790	0.833	-0.118	0.803	-0.420	-0.339	0.612	-0.754	0.754	0.958	1.000			
$\log k'_w$	-0.615	-0.148	0.369	0.922	-0.271	0.126	-0.050	0.816	0.856	-0.105	0.828	-0.404	-0.323	0.604	-0.766	0.766	0.963	0.996	1.000		
$\log k'_{80}$	-0.652	-0.170	0.249	0.889	-0.253	0.102	0.028	0.728	0.775	-0.116	0.750	-0.385	-0.357	0.663	-0.755	0.757	0.928	0.949	0.945	1.000	
I_{CH3}	0.136	0.231	0.113	-0.166	-0.614	0.272	0.683	-0.265	-0.254	-0.214	-0.244	0.077	-0.428	-0.246	0.370	-0.229	-0.087	-0.040	-0.050	0.023	1.000

Table 8

Alignments of the molecules under study



Alignment	Torsion SNNC (°)	Torsion NNCC' (°)	Torsion NCC'C'' (°)	q^2 ^a	NC ^b	SEP ^c
Alignment 1	0	0	0	0.448	2	0.213
Alignment 2	180	0	0	0.419	1	0.214
Alignment 3	0	180	0	0.422	2	0.218
Alignment 4	180	180	0	0.524	3	0.201
Alignment 5	0	180	180	0.407	1	0.216
Alignment 6	180	180	180	0.417	1	0.214
Alignment 7	0	0	180	0.460	2	0.210
Alignment 8	180	0	180	0.455	2	0.211

^a q^2 value after “leave-one-out” cross-validation.^b Number of components.^c Standard error of prediction

Table 9

CoMSIA models

Model	q^2	NC	SEP	r^2 ^a	SEP ^b	<i>F</i> ratio
All fields	0.592	2	0.183	0.700	0.157	29.166
S ^c	0.515	2	0.199	0.681	0.162	26.690
E ^d	0.192	3	0.263	0.510	0.205	8.311
H ^e	0.483	5	0.219	0.711	0.164	10.820
D ^f	0.411	1	0.215	0.456	0.207	21.759
A ^g	−0.101	3	0.307	0.206	0.260	2.079
S+E	0.494	3	0.208	0.682	0.165	17.128
S+H	0.554	5	0.204	0.763	0.149	14.137
S+D	0.545	2	0.193	0.666	0.165	24.910
S+D+E	0.555	3	0.195	0.699	0.160	18.591
S+D+H	0.582	3	0.189	0.710	0.157	19.607
S+D+H+E	0.603	3	0.184	0.728	0.152	21.453
	0.548 ^h			0.753 ⁱ		

^a Explained variance.^b Standard error of estimate.^c Steric field.^d Electrostatic field.^e Hydrophobic field.^f Hydrogen-bond donor field.^g Hydrogen-bond acceptor field.^h q^2_{LHO} value (mean value of 20 runs ‘leave-half-out’ CV).ⁱ $r^2_{bootstrap}$ (mean value of 20 runs).

group in the ligand (or hydrogen-bond acceptor group in the receptor) near the *o*-position. Only compounds **1**, **1h**, **1j**, **4**, **4h** and **4j** have values for the hydrogen-bond donor field different from 0. Among these compounds, only **1h** and **4h** possess *o*-substituent and it is a hydroxy group. So, the *o*-hydroxy substituent increases the antimicrobial activity probably by forming a hydrogen-bond with the target biomacromolecule. Hydrophobic substituents are preferred at *o*- and *p*-positions (Fig. 2, lower left). Negative charged groups are disfavoured at both *o*-positions and favoured at *m*-position (Fig. 2,

lower right). The area of negative potential comprises the dioxol ring of **1k** and **4k** as well.

5. Discussion

From our microbiological results, it is evident that 2-amino-1,2-benzisothiazol-3(2*H*)-ones **1** and **4** both exhibited strong antibacterial activity against several Gram positive and Gram negative bacteria and good antifungal properties. It is worthwhile observing that,

in comparison with 1,2-benzisothiazol-3(2*H*)-one, previously tested by us [24], both of them have a better activity against Gram positive bacteria and SC; only compound **1** is also more active against *E. coli* and *C. tropicalis*. It does demonstrate that the amino group at position 2 of the 1,2-benzisothiazolone ring is effective in improving the intensity of the antimicrobial activity.

In general, the introduction of a 5-methyl substituent on the 2-amino-1,2-benzisothiazol-3(2*H*)-one **1** or the 2-amino condensation with aldehydes leads to derivatives showing comparable or lower antimicrobial properties. The increased antifungal activity observed for compound **11** against *A. niger* (MIC 25 $\mu\text{g mL}^{-1}$) is probably due to the furan moiety, which occurs in several antifungal agents [25].

Chlorosubstitution of compounds **1a** and **4a** did not remarkably enhance the growth inhibitory activity of these substances. However, among **1b–d** and **4b–d**, *para*-substitution was endowed with the better antimicrobial properties.

The **1e–g** and **4e–g** derivatives having the nitrobenzylidene group were devoid of antifungal activity.

The significant difference in activity between the cyclic (**1** and **4**) and the acyclic hydrazide (**2**, **3** and **5**) derivatives indicates that the presence of the 1,2-benzisothiazol-3(2*H*)-one structure is essential to develop antimicrobial properties. According to the hypothetical

mechanism of action, the benzisothiazolone moiety may interact with some proteic thiol groups. This hypothesis was well supported by the observations of Collier et al. [26,27] that the growth inhibitory activity of benzisothiazol-3-one was rapidly quenched by the addition of thiol-containing materials such as glutathione and cysteine. Crossing the outer membrane of the microorganisms could be a limiting step in the antibacterial activity as well [28].

The 2D-QSAR study showed a good correlation between PC1 and the activity against BS, and between PC3 and the activity against SC (Table 7). PC1 correlates with nine of the 14 2D parameters involved in the study. Among them are steric (MVOL, axis *A* and SASA), electrostatic (q_{Nring} and q_{N}) and hydrophobic ($\log P_{\text{calc}}$, $\log k'_{55}$, $\log k'_{80}$ and $\log k'_{\text{w}}$) parameters. Although the high correlation coefficient between activity against BS and q_{Nring} , the explained variance is only 55% when all 28 compounds were included in the correlation.

$$p\text{MIC}_{B.\text{subtilis}} = 15.704(2.778)q_{\text{Nring}} + 10.524(1.024)$$

$$n = 28 \quad r^2 = 0.551 \quad s = 0.188 \quad F = 31.967$$

Any further attempt to improve the correlation by adding other parameters or PCs was unsuccessful. Taking into account the parameters included into PC1 and

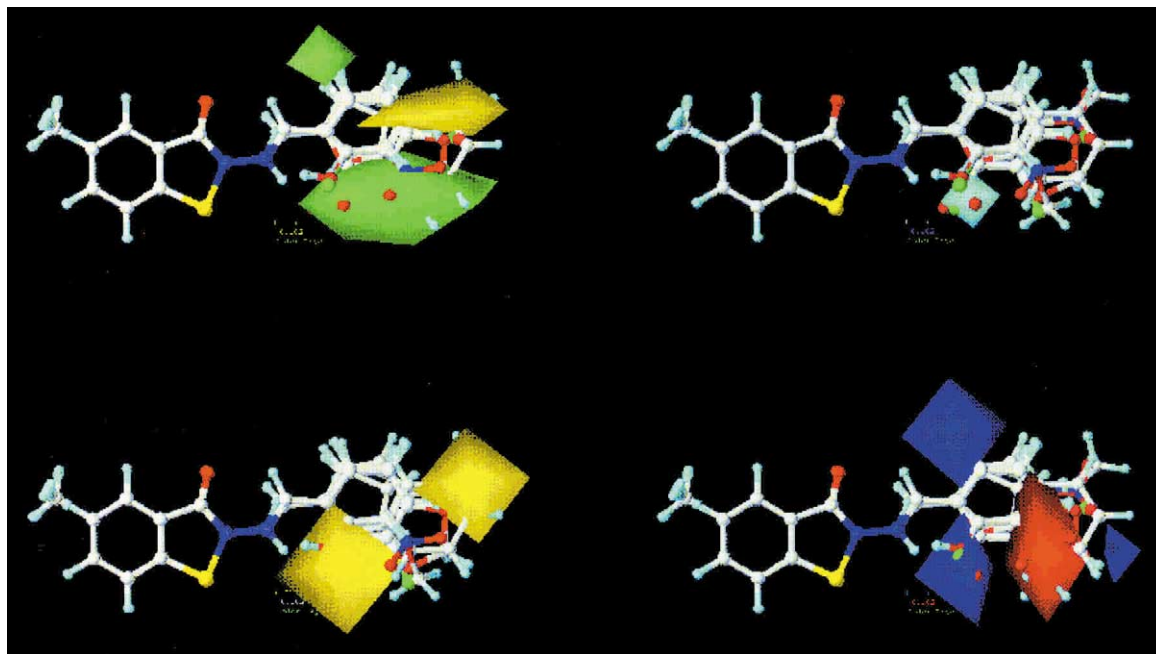


Fig. 2. CoMSIA StDev*Coeff maps contoured by actual values. The aligned structures are shown inside the different fields. The favoured and disfavoured levels are fixed at +0.005 and –0.005, respectively. Upper left: steric map. Green and yellow polyhedra indicate regions where more steric bulk will enhance or reduce, respectively, the activity. Upper right: H-bond abilities. Cyan polyhedron indicates region where hydrogen-bond acceptor group on the receptor (or hydrogen-bond donor on the ligand) will enhance the activity. Disfavoured areas in the hydrogen-bond acceptor map have been not displayed at the accepted level. Lower left: hydrophobic map. Yellow polyhedra indicate regions where hydrophobic groups will enhance the activity. Disfavoured areas in the hydrophobic map have been not displayed at the accepted level. Lower right: electrostatic map. Red and blue polyhedra indicate regions where negative potential will enhance or reduce, respectively, the activity.

their correlation coefficients with activity against BS three interrelated conclusions could be drawn. First, from a steric point of view, substituents with small volume and surface area are preferred. Second, substituents decreasing the positive charge at S and the negative one at N_{ring}, as well as increasing the negative charge at N', will be well accepted electrostatically. Third, substituents with low hydrophobicity will increase the antimicrobial activity. Finally, the presence of CH₃ group at the 5-position of the benzisothiazole ring seems to be insignificant for the activity.

The activity against *S. aureus* correlates well only with axis B: as lower is the value of this parameter, as higher is the activity. The activity against SC depends on PC3. q_O and q_S have the highest scores for this component. Low correlation was found between q_O and this antimicrobial activity.

Further, to outline in details the influence of the substituents on the antimicrobial properties, a 3D-QSAR study was performed using the CoMSIA method.

A CoMSIA model with good predictive power concerning the antimicrobial activity against *B. subtilis* was generated. According to this model four physicochemical properties are important for this activity: steric bulk, hydrogen-bond donor abilities, local hydrophobicity and electrostatic potential. The model reveals preferences for the substituents at *o*-, *m*- and *p*-positions in the phenyl ring as well as the influence of other non-benzylidene substituents on the 2-amino group for the antimicrobial activity. A hydroxy group is well accepted at *o*-position because of its hydrogen-bond formation ability. Bulky negatively charged groups as NO₂ are preferred at *m*-position. At *p*-position are preferred hydrophobic, not very bulky substituents like chlorine. The benzo[1,3]dioxol group contributes positively to the activity because of its negative potential created by the oxygen atoms.

In conclusion some interesting compounds (**1**, **4**, **11**) endowed with antimicrobial activity emerged from the present study. The 1,2-benzisothiazol-3(2*H*)-one moiety is necessary for the studied activity, since the hydrazones of 1,2-benzisothiazolyldhydrazides belonging to series **II**, **III** and **V** are devoid of any antimicrobial effect. Lipophilicity cannot be considered a major factor determining differences in antimicrobial activity, but other physicochemical indices are helpful for the understanding of microbiological results, as shown by our 2D-QSAR and 3D-QSAR analyses.

As the process of antimicrobial activity is not clearly defined in terms of the target biomacromolecules, the QSAR results could not be addressed to a concrete drug-receptor interaction, but they can reveal trends in the relationship between ligand structures and their activities for our set of antimicrobial agents. These trends should prove to be an essential guide to future work in biocides research and development.

6. Experimental

6.1. Chemistry

Melting points °C were determined with a Buchi 512 apparatus and are uncorrected. New compounds were analysed in our analytical laboratory, on a Carlo Erba 1106 Elemental Analyser, for C, H, N. The reactions were followed by TLC on F₂₅₄ silica-gel precoated sheets (Merck) using petroleum ether/ethyl acetate: 1/1 as eluent.

IR spectra were recorded, as KBr pellets, on a JASCO FTIR 300E spectrophotometer (Jasco Ltd., Tokyo, Japan); wave numbers in the IR spectra are given in cm⁻¹. ¹H-NMR (300 MHz) spectra of the newly synthesised compounds, in DMSO-*d*₆ solutions, were recorded on a Bruker AC 300 instrument at 298K. Chemical shifts are reported as δ (ppm) relative to TMS as internal standard; coupling constants *J* are expressed in Hz.

6.1.1. General procedure for synthesis of compounds

1b–m and **4b–m**

The appropriate 2-amino-1,2-benzisothiazol-3(2*H*)-one (**1**, **4**) (5 mmol) was poured in water (70 mL) under stirring and hydrochloric acid added until acidic pH; then the suspension was buffered with sodium acetate and added with ethanol (25 mL). Suitable aldehydes (5.7 mmol) dissolved in ethanol (10 mL) were added to the mixture dropwise, stirring at room temperature for 30 min, for the majority of compounds **1** and for compound **4g**. Compounds **1f**, **1h** and **1j** and all of compounds **4**, except **4g**, required heating, in an oil bath, to 70–80 °C for 1–2 h. The resulting crude product was filtered, washed with water and recrystallised.

2-(2-Chlorobenzylidene)-amino-1,2-benzisothiazol-3(2*H*)-one **1b** IR: ν cm⁻¹ = 3080–3010 (C–H aromatic), 2970, 2850 (C–H aliphatic), 1675 (C=O), 1580 (C=N). ¹H-NMR (300 MHz, DMSO-*d*₆): 8.45 (s, 1H, CH), 8.05–7.98 (m, 3H, H-4,7,3'), 7.79 (t, 1H, *J* = 7.7 Hz, H-5), 7.61–7.48 (m, 4H, H-6,4',5',6').

6.2. Microbiology

New synthesised compounds were evaluated for their in vitro antimicrobial activity against Gram positive, Gram negative bacteria, yeasts and moulds listed in Tables 4 and 6 and compound **11** also against clinical isolates of *A. flavus*, *E. floccosum*, *M. gypseum*, *P. boydii*, *S. schenkii*, *T. interdigitalis*, *T. mentagrophytes*, *T. rubrum* and *T. soudanense*.

The MIC (μ g mL⁻¹) was determined by using the progressive double dilution procedure in liquid or agar medium [29]. The compounds, dissolved in dimethyl sulfoxide, were used in the concentrations range of

0.1–100 $\mu\text{g mL}^{-1}$. The content of dimethyl sulfoxide in any well was 1%. Ampicillin and miconazole were used as reference drugs for antibacterial and antifungal activities, respectively. The compounds were added to the wells containing 10^4 bacteria, 10^3 yeasts or *A. niger* spores into 1 mL of medium (Mueller Hinton broth or Sabouraud liquid medium, respectively). The cells were incubated at 37 °C for 24 h (bacteria) and at 30 °C for 48 h (fungi). Moulds, except *A. niger*, were tested by streaking their suspension on Sabouraud Agar medium containing different concentrations (0.3–100 $\mu\text{g mL}^{-1}$) of the test compounds. The plates were incubated at 25 °C for 14 days. MICs were recorded as the minimum concentration of compound, which inhibits the growth of tested micro-organisms.

The MBC and the MFC were determined by subculturing, on fresh nutrient medium, 20 μL of culture from each tube remained clear. MBC and MFC values represent the lowest concentration of drug required to demonstrate a 99.9% endpoint reduction.

All experiments were performed in triplicate.

6.3. Data analysis

6.3.1. 2D-QSAR

2D parameters were generated as follows: molecular volume MVol, the diameters of the ellipsoid occupied by the molecules axis *A* and axis *B*, the solvent accessible surface area SASA and the dipoles were calculated by [23]; the partial atomic charges q_{O} , q_{S} , q_{Nring} and q_{N} were generated after AM1 single point calculation [30]; $\log P_{\text{calc}}$ and the RP-HPLC parameters $\log k'_{55}$, $\log k'_{80}$ and $\log k'_w$ were taken from [4]. The PCA and MLR analyses were performed by SYSTAT5.02 for Windows [31].

6.3.2. CoMSIA method

The molecular modelling and CoMSIA calculations were performed on a Silicon Graphics octane workstation using SYBYL 6.7 software [32]. The 1,2-benzisothiazole hydrazides were built using the 1,2-benzisothiazole molecule from the SYBYL Standard Fragment Library. Eight different alignments were tested. The compounds of each set were built and MM optimised. The partial atomic charges were computed by AM1 semiempirical method [30] available in the MOPAC v6 implemented in SYBYL.

CoMSIA was performed using the QSAR option of SYBYL. Five physicochemical properties (steric, electrostatic, hydrophobic, and hydrogen-bond donor and acceptor) were evaluated, using a common probe atom with 1 Å radius, charge +1, hydrophobicity +1, hydrogen-bond donor and acceptor properties +1. Similarity indices were calculated using Gaussian-type distance dependence between the probe and the atoms of the molecules of the data set, according to the equation:

$$A_q(j) = \sum w_{\text{probe},k} w_{ik} e^{-\alpha r_{iq}^2}$$

where *A* is the similarity index at grid point *q*, summed over all atoms *i* of the molecule *j*, $w_{\text{probe},k}$ the probe atom, w_{ik} the actual value of the physicochemical property *k* of atom *i*, r_{iq} the mutual distance between the probe at grid point *q* and atom *i* of the test molecule, α an attenuation factor. Different values of the attenuation factor α were tested. These values ranged from 0.1 to 1.2 in incremental steps of 0.1.

PLS methodology was used for the 3D-QSAR analysis. The grid extended beyond the molecular dimensions by 2.0 Å in all directions. Different resolution steps were tested: 1.0, 1.5, 2.0, 2.5 and 3.0 Å. Different column filterings σ_{min} (from 0.0 to 4.0 with a step of 0.5) were analysed as well. σ_{min} indicates which grid points to include in the analysis, for example $\sigma_{\text{min}} = 2.0$ indicates that columns (similarity indices) whose variance is less than 2.0 are omitted.

The predictive power of the models was assessed by the cross-validated coefficient q^2 and the standard error of prediction (SEP):

$$q^2 = 1 - \frac{\text{PRESS}}{\text{SSQ}}$$

$$\text{SEP} = \sqrt{\frac{\text{PRESS}}{p-1}}$$

where PRESS is the predictive sum of squares ($\sum_{i=1}^n (p\text{MIC}_{\text{exp}} - p\text{MIC}_{\text{pred}})^2$), SSQ the sum of squares of $p\text{MIC}_{\text{exp}}$ corrected for the mean ($\sum_{i=1}^n (p\text{MIC}_{\text{exp}} - p\text{MIC}_{\text{mean}})^2$), *p* is the number of the peptides omitted, and $p\text{MIC}_{\text{pred}}$ is the value predicted by 'leave-one-out' CV. CV is performed by dividing the data into a number of groups, developing a number of parallel models from the reduced data with one of the groups omitted, and then predicting the biological activities of the excluded compounds. When the number of the groups omitted is equal to the number of the compounds in the set, the procedure is called 'leave-one-out' CV (LOO-CV). More robust CV test, using two groups ('leave-half-out'), was performed to estimate the extent of chance correlation in the model. The mean of 20 runs is given as q^2_{LHO} .

The optimum number of components (NC) used to derive the non-cross-validated model was defined as the number of components leading to the highest q^2 and the lowest SEP. The non-cross-validated models were assessed by the explained variance r^2 , standard error of estimate (SEE), and *F* ratio. A bootstrap analysis [33] was performed in 20 runs for the best model and the mean r^2 is given as $r^2_{\text{bootstrap}}$. This model was used to display the coefficient contour maps.

The visualisation of the results of the CoMSIA analyses has been performed using the 'StDev*Coeff' mapping option contoured by actual values. Favoured

and disfavoured levels fixed at $+0.005$ and -0.005 , respectively, were used for all fields. The contours of the CoMSIA steric map are shown in green (more bulk is favoured) and yellow (less bulk is favoured). The electrostatic map are in red (negative potential is favoured) and blue (negative potential is disfavoured) contours. CoMSIA hydrophobic fields are coloured in yellow (hydrophobic groups enhance activity) and white (hydrophobic groups decrease activity). The hydrogen-bond field contours show regions where hydrogen-bond donors on the ligand (hydrogen-bond acceptors on the receptor) will enhance (cyan) or reduce (purple) the antimicrobial activity.

Acknowledgements

This work was supported by research grants FIL 2001-University of Parma, Italy. The authors would like to thank Dr. Darren Flower, Jenner Institute, for the helpful discussion.

References

- [1] F. Zani, P. Vicini, *Arch. Pharm. Pharm. Med. Chem.* 331 (1998) 219–223.
- [2] P. Vicini, F. Zani, *Il Farmaco* 52 (1997) 21–24.
- [3] P. Vicini, P. Mazza, *Il Farmaco* 44 (1989) 511–517.
- [4] P. Vicini, E. Fisicaro, M.T. Lugari, *Arch. Pharm. Pharm. Med. Chem.* 333 (2000) 135–144.
- [5] M.E. Abdel-Fattah, E.E. Salem, M.A. Mahmoud, *Ind. J. Heteroc. Chem.* 10 (2000) 121–128.
- [6] S. Ersan, S. Nacak, R. Berkem, T. Özden, *Arzneim-Forsch/Drug Res.* 47 (1997) 963–965.
- [7] I. Yildir, H. Perçiner, M. Fethi Sahin, U. Abbasoglu, *Arch. Pharm.* 328 (1995) 547–549.
- [8] Z. Cesur, S. Büyüktimkin, N. Büyüktimkin, *Arch. Pharm.* 323 (1990) 141–144.
- [9] F. Vittorio, G. Ronsisvalle, A. Marrazzo, G. Blandini, *Il Farmaco* 50 (1995) 265–272.
- [10] A. De, in: G.P. Ellis, G.B. West (Eds.), *Progress in Medicinal Chemistry*, Elsevier, North-Holland Biomedical Press, 1981, pp. 117–133.
- [11] M. Davis, in: A.R. Katritzky, A.J. Boulton (Eds.), *Advances in Heterocyclic Chemistry*, Academic Press, New York, 1985, pp. 114–116.
- [12] P. Borgna, M.L. Carmellino, M. Natangelo, G. Pagani, F. Pastoni, M. Pregnolato, M. Terreni, *Eur. J. Med. Chem.* 31 (1996) 919–925.
- [13] T. Okada, K. Ezumi, M. Yamakawa, H. Sato, T. Tsuji, T. Tsushima, K. Motokawa, Y. Komatsu, *Chem. Pharm. Bull.* 41 (1993) 126–131.
- [14] M.S. Tute, in: J.G. Topliss (Ed.), *Quantitative Structure–Activity Relationships of Drugs*, Academic Press, New York, 1983, p. 23 ff.
- [15] S.J. Fuller, S.P. Denyer, W.B. Hugo, D. Pemberton, P.M. Woodcock, A.J. Buckley, *Lett. Appl. Microbiol.* 1 (1985) 13–15.
- [16] M.L. Carmellino, G. Pagani, M. Pregnolato, M. Terreni, F. Pastoni, *Eur. J. Med. Chem.* 29 (1994) 743–751.
- [17] T. Hashiguchi, T. Itoyama, A. Kodama, K. Uchida, H. Yamaguchi, *Arzneim-Forsch/Drug Res.* 47 (1997) 1218–1221.
- [18] Y. Wahbi, C. Tournaire, R. Caujolle, M. Payard, M.D. Linas, J.P. Seguela, *Eur. J. Med. Chem.* 29 (1994) 701–706.
- [19] G. Klebe, U. Abraham, T. Mietzner, *J. Med. Chem.* 37 (1994) 4130–4146.
- [20] G. Klebe, U. Abraham, *J. Comput. Aid. Mol. Des.* 13 (1999) 1–10.
- [21] M. Böhm, J. Stürzebecher, G. Klebe, *J. Med. Chem.* 42 (1999) 458–477.
- [22] P. Vicini, L. Amoretti, M. Tognolini, V. Ballabeni, E. Barocelli, *Bioorg. Med. Chem.* 8 (2000) 2355–2358.
- [23] A. Nicholls, K. Sharp, B. Honig, *Proteins, Structure, Function and Genetics*, vol. 11, o. 4, 1991, p. 281 ff.
- [24] G. Massimo, F. Zani, E. Coghi, A. Bellotti, P. Mazza, *Il Farmaco* 45 (1990) 439–446.
- [25] E. Grunberg, E.H. Tittsworth, *Ann. Rev. Microbiol.* 27 (1973) 317–346.
- [26] P. Collier, A. Ramsey, P. Austin, P. Gilbert, *J. Appl. Bacteriol.* 69 (1990) 569–577.
- [27] P. Collier, A. Ramsey, R. Waigh, K. Douglas, P. Austin, P. Gilbert, *J. Appl. Bacteriol.* 69 (1990) 578–584.
- [28] M. Mor, F. Zani, P. Mazza, C. Silva, F. Bordini, G. Morini, P. Plazzi, *Il Farmaco* 51 (1996) 493–501.
- [29] J.H. Jorgensen et al., in: P.R. Murray, E.J. Baron, M.A. Pfaller, F.C. Tenover, R.H. Tenover (Eds.), *Manual of Clinical Microbiology*, American Society of Microbiology, Washington, DC, 1995, pp. 1275–1341 and 1405–1414.
- [30] M. Dewar, E. Zebisch, E. Healy, J. Stewart, *J. Am. Chem. Soc.* 107 (1985) 3902–3909.
- [31] SYSTAT 5.02 for Windows. SYSTAT Inc., 1800 Sherman Ave., Evanston, IL 60201.
- [32] SYBYL 6.7. Tripos Inc, 1699 Hanley Road, St Louis, MO 63144.
- [33] R. Cramer, J. Bunce, D. Patterson, *Quant. Struct.–Act. Relat.* 7 (1988) 18–25.